Arrested fungal biofilms as low-modulus structural biocomposites: Water holds the key

R. Aravinda Narayanan[1]* and Asma Ahmed[2]

[1]Department of Physics, Birla Institute of Technology and Science (Pilani), Hyderabad campus, Hyderabad - 500078, India
E-mail: raghavan@hyderabad.bits-pilani.ac.in
*Corresponding author

[2]School of Human and Life Sciences,
Canterbury Christ Church University, North Holmes Road Canterbury, CT1 1QU, United Kingdom

ABSTRACT

Biofilms are self-assembling structures consisting of rigid microbial cells embedded in soft biopolymeric extracellular matrix (ECM), and have been commonly viewed as being detrimental to health and equipment. In this work, we show that biofilms formed by a non-pathogenic fungus *Neurospora discreta*, are fungal bio-composites (FBCs) that can be directed to self-organize through active stresses to achieve specific properties. We induced active stresses by systematically agitating the reactor between 0 and 150 RPM during the growth of FBCs. By growing FBCs that are strong enough to be conventionally tensile loaded for the first time, we find that as agitation rate increases, the elongation strain at break of the FBCs increases linearly, and their elastic modulus correspondingly decreases. Using results from microstructural imaging and thermogravimetry, we rationalize that agitation increases the production of ECM, which concomitantly increases the water content of agitated FBCs up to 250% more than un-agitated FBCs. Water held in the nanopores of the ECM acts a plasticizer and controls the ductility of FBCs in close analogy with polyelectrolyte complexes. This paradigm shift in viewing biofilms as bio-composites opens up the possibility for their use as sustainable, biodegradable, low-modulus structural materials.

1. Introduction

Microorganisms such as bacteria and fungi, as an evolutionary survival instinct, fortify themselves by collectively organizing at interfaces and secreting an extracellular biopolymeric matrix (ECM) to form composite structures such as films, mats, flocs and sludge, which are known as biofilms[1,2]. They can be viewed as complex fluids as they are made of relatively brittle microbial cells akin to colloidal particles embedded in a matrix of self-produced cross-linked ECM[3]. The ECM is an entangled mixture of polysaccharides, proteins, lipids, nucleic acids. The cells and the ECM are in a highly hydrated environment and form an intricate porous network that enables nutrient transport as well as water retention[1].

The microscopic structure of a biofilm is linked to its viscoelasticity, which has an important function - the elastic part provides mechanical stability to the three-dimensional architecture, while the viscous part allows it to expand as the cells multiply, and also helps to absorb environmental stresses[4–6].

Although some biofilms are beneficial, research on biofilms has largely focused on the hazardous nature of biofilm-cells borne out of their 'resistivity to biological, chemical and physical assaults'[7]. The implication is that by attaching to surfaces they can spread infectious diseases[8]; corrode and foul industrial equipments causing huge economic losses[9]. Therefore, biofilm mechanics is studied to understand their adhesive properties so as to develop strategies for their detachment from surfaces[6,10]. However, owing to the structural fragility of biofilms whose elastic modulus is a few kPa, conventional tensile testing has not been possible [11].

Instead, many unconventional *in-situ* mechanical testing methods have been devised[12–17], and to this day mechanical characterization of biofilms remains non-standardized[18].

Biofilms are a form of *active matter*[19] in which energy is transduced to increase the biomass – both cells and the ECM - with the aid of several factors which include nutrients, pH, inoculum size, temperature and flow conditions. As the biofilm grows over many days it undergoes several stages of growth, which are distinguished by biomass growth rates[2]. Ultimately after the exhaustion of the supplied nutrient, the biofilm begins consuming the self-produced ECM and disintegrates. Viewed through statistical mechanical principles, during growth, the active matter explores several dynamical states in the potential energy hypersurface[20] with the help of active stresses which are essentially local forces generated through cell division and cellular motion [21]: The structures of such soft solids are stabilized by these internal stresses which account for their shear rigidity at length scales much bigger than atomic scales[22].

Given their intricate microstructure and unique mechanical properties[1], the question arises: Can biofilms be viewed as biomaterials, their properties altered and used in applications? In general, biomaterials, through hierarchical arrangement of brittle and ductile components present in them, naturally form bio-composites [23,24]. A recent strategy has been to tune the mechanical properties of such bio-composites by varying the growth conditions, circumventing the need for expensive processing conditions[25]: As an example, it was shown that fungal mycelia grown on two bio-substrates (nutrients) that are distinguished by the ease of digestion, exhibited different mechanical properties which could be traced to the relative concentrations of brittle and ductile structural components[25]. Hence, the motivation for the present study is

to establish structure-property relationships in biofilms to enable their use as biodegradable and sustainable biomaterials.

In this study, we grew non-pathogenic air-liquid interface fungal biofilms using *Neurospora discreta*, which are referred to as fungal bio-composites (FBCs), under controlled agitated growth conditions, which enabled tuning of their mechanical properties from brittle to ductile. We explored how energy supplied across the boundary of the system through agitation, affected the microstructure. Here, an important difference between biofilms formed by fungi and bacteria should be noted, especially since in the physics literature biofilms are synonymous with bacterial biofilms where motility of bacteria is one of the ways in which active stress is generated[19,26]. On the contrary, in fungal biofilms, the cells are filamentous and non-motile[2]: They generate active stresses while growing in length and branching. We harvested the FBCs from the reactor for further investigations at a point in time during their growth when the supplied nutrients are about to be exhausted: The active matter was thus "frozen" in one of the dynamical states, as it no longer had access to nutrients and hence could not grow. A highlight is that the FBCs were strong enough to be conventionally tensile loaded, for the first time, which is a relevant test for structural applications. Furthermore, in contrast to biofilms formed on liquid-solid interfaces, as these FBCs grow on the air-liquid interface, they can be harvested easily without damaging their structure. One of the key findings of this work is that water, accounting for 90% by weight of the FBCs, held in micron and nano-sized pores in the ECM determines their mechanical strength. This new view of biofilms, as low elastic modulus materials can pave the way for potential applications in soft biomedical devices, tissue engineering constructs, and bio-membranes for wastewater treatment.

2. Experimental

2.1 Biofilm growth

Fungal bio-composites were grown aseptically in 250 ml Erlenmeyer flasks (Fig. 1) containing 100 ml Vogel's minimum medium [27] with 2% sucrose, using a locally isolated non-pathogenic filamentous fungus *Neurospora discreta*. The inoculum was prepared by scraping cells from the potato dextrose agar plates on which they were maintained, and suspending them into a small volume of sterile medium. One milliliter (ml) of the spore suspension was then added to each flask, at a concentration of 2.5×10^6 cells/ml. After initial mixing, the flasks were incubated at 30^0C and a fully formed layer of the FBC on the air-liquid interface was observed in about 48 hours. Duplicate sets of flasks were then transferred to separate incubator shakers set at 30^0C and agitated at 60 RPM (revolutions per minute), 100 RPM, and 150 RPM, respectively, apart from growing biofilms without agitation which we refer to in this article as 'static FBC'. The FBCs were harvested after 7 days of growth which is well into the exponential growth rate phase and just before the stationary phase[2]. After removing from the air-liquid interface, the FBCs were placed on a grade-I Whatman filter paper for about ten minutes to drain excess medium. The wet weights of the FBCs, a measure of capacity to hold water, were then recorded. The surface of the FBCs were sprayed with isopropyl alcohol to arrest further cell growth and then refrigerated in sealed petri dishes at 2-4^0C until further analysis.

2.2 Characterization of fungal biocomposites

Thermogravimetric analysis (TGA) was performed on the samples using DTG-60 Shimadzu thermal analyzer in nitrogen atmosphere by heating from 30 ^{0}C to 800 ^{0}C at a ramp rate of 10^0C

per minute. The stress versus strain curves for the FBCs were measured at a constant temperature of 28^0C, using DMA (TA-Q800) in the film-tension geometry at a stress ramp rate of 0.1 N/minute, until the sample structurally failed. For the DMA experiments, the samples were cut to a rectangular shape with a length of ~20 mm and width of ~ 8mm. Thickness of samples varied between 1-3 mm.

FBCs surface morphology was characterized using Field Emission Scanning Electron Microscopy (FESEM) using FEI (Apreo S): Analysis of the images was performed using the *imageJ* software and the plugin *OrientationJ* to determine the filament orientation distribution[28]. FBCs microstructure across the different stacked layers was characterized by confocal laser scanning microscopy (CLSM) using Leica DMi8 inverted microscope. Bright-field image stacks were obtained with a 40X oil objective with z-step of 1 micrometer. COMSTAT software[29] was used to analyze the CLSM images to calculate diffusion distance, defined as the length of the shortest path from a voxel - a 3D pixel - inside the biomass to the void: When this quantity is averaged over all the voxels in a slice, average diffusion distance is obtained which is used in further analysis. For all microscopic investigations, the samples were dried for 48 hours at 28-30^{o}C.

3. Results and Discussion

In comparison to static FBC, those grown under agitation swelled by absorbing water in the range of 60% to 250%, as calculated from the order of magnitude differences in their wet weights (Table 1). There are two underlying connected mechanisms that explain the increase in wet weight of FBCs due to agitation: (1) *Shear stress* - studies have indicated that shear stress on a growing biofilm causes greater production of ECM[30], and in particular, the polysaccharides. The soluble component of the ECM is the polysaccharide which soaks up and

retains water[31]; (2) *Mass transfer* - Biomass production depends on the ability of the nutrients to reach the cells which is severely diffusion limited[32]. This situation could be altered if advection is introduced. Theoretically, it has been shown that even in the absence of external forces a collection of microorganisms can engender coherent transport arising due to gradients in density or activity[26]. In our experiment, the externally imparted shear force causes advective transport of the nutrients and concomitantly deforms the FBCs, setting up additional local nutrient gradients in density and activity. The momentum transferred by agitation to the FBCs which causes their deformation can be quantified through Reynolds number (*Re*). In un-baffled 250 ml Erlenmeyer flasks, in which the FBCs were grown, *Re* for 60 RPM, 100 RPM, 150 RPM is calculated[1] to be 26,000, 44,000, and 64,000, respectively: In these flasks turbulent flow onsets[33] for *Re* of about 60,000. Due to the flow conditions surface texture of the FBCs grown at 100 RPM and 150 RPM were visibly anisotropic. At 150 RPM we obtained structurally fragmented FBCs which could not be tensile loaded. The 60 RPM FBCs were visibly smooth and it should be noted that they were grown the farthest from the turbulent regime among the agitated samples.

The capacity of the FBCs to retain water is measured through thermogravimetry that showed single step decomposition whose initial temperature is about 40^0C and the final temperature is about 140^0C (Fig. 2). This decomposition is attributed to the loss of water and provides evidence that water constitutes nearly 90% by weight of the FBCs. Further analysis of the TGA

[1] $Re=(2r^2 \omega\rho)/\eta$, where the radius of the biofilm (r) ≅4 cm and the angular velocity (ω) $= \frac{2\pi \times RPM}{60}$.

At 30^0C, density of water (ρ) = 996 kg.m^{-3} and viscosity of water (η) = 0.8 mPa.s.

plots shows that the temperature range of water loss, which signifies thermal stability is greater for the agitated FBCs. Interestingly, the rate of water loss does not show a monotonic trend with agitation with the 60 RPM sample exhibiting the least rate of water loss (Table 1).

Water is held in pores which are contiguous and provide the channel for the transport of nutrients[31]. Pores are the space between the crisscrossing filaments. FESEM images reveal that static and agitated growth conditions lead to distinctly different microstructures (Fig. 3): They represent frozen active matter arrested in different dynamical states which are influenced by filament length, filament orientation, and the ECM. In the static FBC, the filamentous cells are long and curved with the longest visible filament measuring about 60 µm. In the agitated samples, the longer filaments are relatively straight and along with that progressively shorter filaments can be observed with increasing agitation. In the 150 RPM sample, the filament size is only about 6 µm. All the samples show similar angular distribution of filaments with prominent peaks at 0^0, 45^0, and -45^0: The angle between the 'x'-axis and the positive 'y'-axis is 90^0 and at the other extreme, the angle between the 'x'-axis and the negative 'y'-axis is -90^0. The images also reveal increased production of ECM around the filaments, in the growing end of the filaments (bulbous growth in 100 RPM) and in the space between the filaments. We explain these observations as follows: *Filament length* - Due to their non-motile nature, fungal hyphae grow in length, seeking nutrients. However, with increasing agitation, due to greater mass transfer, filaments need not grow as much to access the nutrients. *Filament orientation* - The filaments are positionally disordered but orientationally ordered in a narrow angular range indicating a nematic liquid-crystal like ordering[21]. *Production of ECM* – The energy released by the hydrolyzed ATP can be used by the system for filament growth and ECM production. In

the agitated samples, this energy is mainly used in the greater production of ECM which is also corroborated by their greater wet weights. While agitation, in general, helps ECM production, the capacity to retain water and the rate of water loss are influenced by the size and distribution of pores which, our present study indicates is determined by the filament length.

Confocal laser scanning microscopy provides another dimension to this picture: sliced bright-field images of the sample are obtained in the z-direction which are then stacked and reconstructed to produce a three dimensional view of the pores and their contiguous nature (Fig. 4). Biomass interspersed with pores makes the FBCs spatially heterogeneous. We define spatial heterogeneity, which quantifies the order at micrometer length scales as $\Delta_d = D_i - \langle D \rangle_{all\ slices}$, where D_i is the average diffusion distance in a given slice, and $\langle D \rangle_{all\ slices}$ is the average of D_i over all the slices (Fig. 5). D_i is a measure of distances over which the nutrients are transported which affects the formation of the FBCs[29]. If Δ_d is less than zero, it implies that in a given slice, the diffusion distance is less than the average diffusion distance of the whole composite: In other words the areal porosity is higher in that slice. The FBCs in this study grow by floating on the air-liquid interface to overcome the depletion of dissolved oxygen in the liquid medium[7]: At the air-FBC interface aerial filaments shoot up to absorb oxygen from air. At this interface the concentration of filaments is more than the ECM, and therefore, $\Delta_d < 0$ and is called ECM-depleted region. For the agitated FBCs, note that Δ_d is less negative at the air-liquid interface because of better transport of dissolved oxygen to the cells. At a depth of a few micrometers from the air-liquid interface, Δ_d switches to positive values implying an ECM-rich region. The two 'micro-structural phases' ($\Delta_d < 0$ and $\Delta_d > 0$) percolate into the FBCs as it self-organizes layer by layer as predicted by computer simulation studies[34].

Now, we discuss the central theme of this article – the mechanical properties of the FBCs. The static FBC exhibited brittle behavior, as seen in the nearly linear relationship between stress and strain, before mechanical failure at nearly 20% elongation (Fig. 6). This elastic region shrinks considerably in the agitated FBCs, where we observe that for approximately 3% strain, the slope sharply decreases but the sample continues to stretch with increasing load. The elongation at break is relatively higher at 27% and 37%, respectively for the 60 RPM and 100 RPM samples, respectively, signifying ductile behavior. While the elastic modulus (*E*) of the FBCs obtained from the initial elastic region is in excess of 100 kPa which compares well with values obtained from compressive testing of *C. albicans* fungal biofilms[35] and an order of magnitude greater than that reported for bacterial biofilms[11]. However, the shear thinning response under agitation seen in the present study is uncommon[4] which along with relatively higher elastic modulus enabled the tensile testing of the FBCs.

To understand the structure – mechanical property correlations we invoke a deep analogy with a class of materials called polyelectrolyte complexes[36,37] (PECs) which share many attributes with FBCs. The composition of PECs is polycations and polyanions which adsorb on solid surfaces and interact with each other to form multilayered film. Their mechanical properties are linked to the composition, porosity, and capacity to retain water. Here, in FBCs the water and nutrients are transported through micro- and nano-pores[38,39]. These pores act as membranes which are impermeable to macromolecules such as polysaccharides. With agitation during growth, as production of ECM increases, the concentration gradient of macromolecules increases – osmotic pressure – resulting in uptake of water through the pores to reduce the gradient. As the cross-linked ECM swells with water, it exerts opposing mechanical pressure and

helps in establishing equilibrium[31]. The water held in the ECM impacts the mechanical properties of FBCs as follows: Suppose that there is no water in the ECM, then the repulsive interactions between polyanionic macromolecules are stabilized through counterions which act as a bridge between them[37]. It is known that ionic interactions between negatively charged polysaccharides and say, Ca^{2+} in the ECM densifies and stabilizes the ECM[40]. In this process, the macromolecules lose their flexibility to become stiff which translates into macroscopic brittle behavior. On the other hand, in the presence of water, both the intra-chain repulsive interactions in a polysaccharide macromolecule and attractive counterion interactions between polysaccharide macromolecules are screened, creating more free volume, consequently increasing the flexibility of the macromolecules explaining the reduction in elastic modulus and increasing elongation at break in agitated FBCs. In line with polyelectrolyte complexes, we interpret the stress versus strain plot of FBCs as due to two processes[36]. The larger *E* (greater than 100 kPa) for small strains is attributed to a flow independent mechanism occurring due to a relatively faster relaxation of the filament network which also encompasses the micropores. The smaller *E* (less than100 kPa) which is observed in agitated FBCs is associated with a flow dependent mechanism involving the slower relaxation of water in the nanopores. As mentioned earlier, the equilibrium at the porous membrane through which water flows is established with the help of cross-linked ECM. Here, the interaction is largely entropic and the elastic shear modulus (G_e) is determined[41] by the relationship, $G_e \approx \frac{k_B T}{\xi^3}$, where ξ, denotes the ECM polymer entanglement mesh size and k_B is the Boltzmann constant. Using the value of *E* rom the smaller slope in the agitated FBCs at $T = 28^0 C$, we estimate that ξ is between 2-5 nm. This

theoretical prediction is confirmed by FESEM (Fig. 7) which reveals the presence of nanopores embedded in the ECM.

4. Conclusion

Biofilms have previously been characterized as complex fluids[3] and as active matter[19], but this study presents a unique materials view of biofilms as biocomposites. We have shown that agitated growth is a key process lever, which impacts the microstructure of FBCs and their ability to retain water in pores. Water acts as a plasticizer which helps in tuning the mechanical properties of FBCs. The micro-environment of the ECM in FBCs, their elastic modulus in the range of kPa, and their membranous structure will enable applications in soft biomedical devices [42,43], tissue engineering constructs [44], and bio-membranes for wastewater treatment[45]. The analogy with the well-studied polyelectrolyte complexes will help in further optimizing the properties of FBCs by choosing external variables like osmotic stressing agents and ionicity of the growth medium. FBCs can also serve as model systems to study glassy state in active matter[46]. The glassy state is characterized by the onset of dynamical heterogeneities and this study indicates that water increases the free volume and allows the FBCs to explore different dynamical states resulting in a brittle-to-ductile transition.

Acknowledgements

The authors thank the central analytical lab facility and the Department of Physics facility at BITS (Pilani), Hyderabad campus for access to confocal microscopy, FESEM and DMA.

Author Contribution Statement

AA performed the biofilm growth experiments, RAN performed the characterization studies.
Both authors contributed to the interpretation of the data.

References

1. H. C. Flemming and J. Wingender, Nat. Rev. Microbiol. **8**, 623 (2010).

2. A. P. J. Moore, D., Robson, G.D., Trinci, *21st Century Guidebook to Fungi* (Cambridge University Press, Cambridge, UK, 2011).

3. J. N. Wilking, T. E. Angelini, A. Seminara, M. P. Brenner, and D. A. Weitz, Mater. Res. Soc. **36**, 385 (2011).

4. M. G. Mazza, J. Phys. D. Appl. Phys. **49**, 203001 (2016).

5. T. Shaw, M. Winston, C. J. Rupp, I. Klapper, and P. Stoodley, Phys. Rev. Lett. **93**, 98102 (2004).

6. V. D. Gordon, M. Davis-fields, and K. Kovach, J. Phys. D. Appl. Phys. **50**, 223002 (2017).

7. M. Morikawa, J. Biosci. Bioeng. **101**, 1 (2006).

8. B. Li and T. J. Webster, J. Orthop. Res. **36**, 22 (2018).

9. C. C. C. R. De Carvalho, Front. Mar. Sci. **5**, 1 (2018).

10. N. Billings, A. Birjiniuk, T. S. Samad, and P. S. Doyle, Reports Prog. Phys. **78**, 36601 (2015).

11. M. Böl, A. E. Ehret, A. Bolea Albero, J. Hellriegel, and R. Krull, Crit. Rev. Biotechnol. **33**, 145 (2013).

12. A. Ohashi and H. Harada, Water Sci. Technol. **29**, 281 (1994).

13. P. Stoodley, R. Cargo, C. J. Rupp, S. Wilson, and I. Klapper, J. Ind. Microbiol. Biotechnol. **29**, 361 (2002).

14. D. N. Hohne, J. G. Younger, and M. J. Solomon, Langmuir **25**, 7743 (2009).

15. F. Quilès, S. Saadi, G. Francius, J. Bacharouche, and F. Humbert, Biochim. Biophys. Acta **1858**, 75 (2016).

16. S. Grumbein, M. W. O. Lieleg, S. Grumbein, and M. Werb, J. Rheol. (N. Y. N. Y). **60**, 1085 (2016).

17. L. I. Brugnoni, M. C. Tarifa, J. E. Lozano, and D. Genovese, Biofouling **30**, 1269 (2014).

18. H. Boudarel, J. D. Mathias, B. Blaysat, and M. Grédiac, Npj Biofilms Microbiomes **4**, 17 (2018).

19. Y. I. Yaman, E. Demir, R. Vetter, and A. Kocabas, Nat. Commun. **10**, 2285 (2018).

20. D. J. Wales, *Energy Landscapes* (Cambridge University Press, Cambridge, UK, 2003).

21. D. Needleman and Z. Dogic, Nat. Rev. Mater. **2**, (2017).

22. S. Alexander, Phys. Rep. **296**, 5 (1998).

23. K. Tai, M. Dao, S. Suresh, A. Palazoglu, and C. Ortiz, Nat. Mater. **6**, 454 (2007).

24. G. Tudryn, L. Schadler, R. C. Picu, M. R. Islam, and R. Bucinell, Sci. Rep. **7**, 1 (2017).

25. M. Haneef, L. Ceseracciu, C. Canale, I. S. Bayer, J. A. Heredia-Guerrero, and A. Athanassiou, Sci. Rep. **7**, 41292 (2017).

26. A. J. T. M. Mathijssen, F. Guzmán-Lastra, A. Kaiser, and H. Löwen, Phys. Rev. Lett. **121**, 248101 (2018).

27. H. J. Vogel, Am. Nat. **XCVIII**, 435 (1964).

28. R. Rezakhaniha, A. Agianniotis, J. T. C. Schrauwen, A. Griffa, D. Sage, C. V. C. Bouten, F. N. Van De Vosse, M. Unser, and N. Stergiopulos, Biomech. Model. Mechanobiol. **11**, 461 (2012).

29. A. Heydorn, A. T. Nielsen, M. Hentzer, M. Givskov, B. K. Ersbøll, and S. Molin, Microbiology **146**, 2395 (2000).

30. P. Stoodley, R. Cargo, C. J. Rupp, S. Wilson, and I. Klapper, J. Ind. Microbiol. Biotechnol. **29**, 361 (2002).

31. W. D. Comper, R. P. W. Williams, and O. Zamparo, Connect. Tissue Res. **25**, 89 (1990).

32. P. S. Stewart, J. Bacteriol. **185**, 1485 (2003).

33. C. P. Peter, Y. Suzuki, and J. Bu, Biotechnol. Bioeng. **93**, 1164 (2006).

34. P. Ghosh, J. Mondal, E. Ben-Jacob, and H. Levine, Proc. Natl. Acad. Sci. **112**, E2166 (2015).

35. E. Paramonova, B. P. Krom, H. C. van der Mei, H. J. Busscher, and P. K. Sharma, Microbiology **155**, 1997 (2009).

36. H. H. Hariri and J. B. Schlenoff, Macromolecules **43**, 8656 (2010).

37. H. H. Hariri, A. M. Lehaf, and J. B. Schlenoff, Macromolecules **45**, 9364 (2012).

38. D. De Beer, P. Stoodley, and Z. Lewandowski, Biotechnol. Bioeng. **44**, 636 (1994).

39. A. Birjiniuk, N. Billings, E. Nance, J. Hanes, K. Ribbeck, and P. S. Doyle, New J. Phys. **16**, 85014 (2014).

40. H. C. Flemming and J. Wingender, Nat. Rev. Microbiol. **8**, 623 (2010).

41. M. Rubinstein and R. H. Colby, *Polymer Physics* (Oxford University Press, NY, 2003).

42. K. Jang, H. U. Chung, S. Xu, C. H. Lee, H. Luan, J. Jeong, H. Cheng, G. Kim, S. Y. Han, J. W. Lee, J. Kim, M. Cho, F. Miao, Y. Yang, H. N. Jung, M. Flavin, H. Liu, G. W. Kong, K. J. Yu, S. Il Rhee, J. Chung, B. Kim, J. W. Kwak, M. H. Yun, J. Y. Kim, Y. M. Song, U. Paik, Y. Zhang, Y. Huang, and J. A. Rogers, Nat. Commun. **6**, 1 (2015).

43. S. Raghavan, N. Fernandes, and B. Cipriano, Gels **4**, 18 (2018).

44. L. R. Madden, D. J. Mortisen, E. M. Sussman, S. K. Dupras, J. A. Fugate, J. L. Cuy, K. D. Hauch, M. A. Laflamme, C. E. Murry, and B. D. Ratner, Proc. Natl. Acad. Sci. **107**, 15211 (2010).

45. A. Mohamed El-hadi and H. Alamri, Polymers (Basel). **10**, 1174 (2018).

46. R. Mandal, P. J. Bhuyan, P. Chaudhuri, M. Rao, and C. Dasgupta, Phys. Rev. E **96**, 42605 (2017).

Table

Table 1. Water holding capacity and water loss of the FBCs

Sample	Wet weight (g)	Range of water loss (^{0}C)	Rate of water loss (mg/^{0}C)
Static	5.53 ± 1.08	60	2.9
60 RPM	19.53 ± 4.48	110	2.3
100 RPM	16.60 ± 2.67	110	2.6
150 RPM	9.08 ± 0.91	110	3.0

Figures

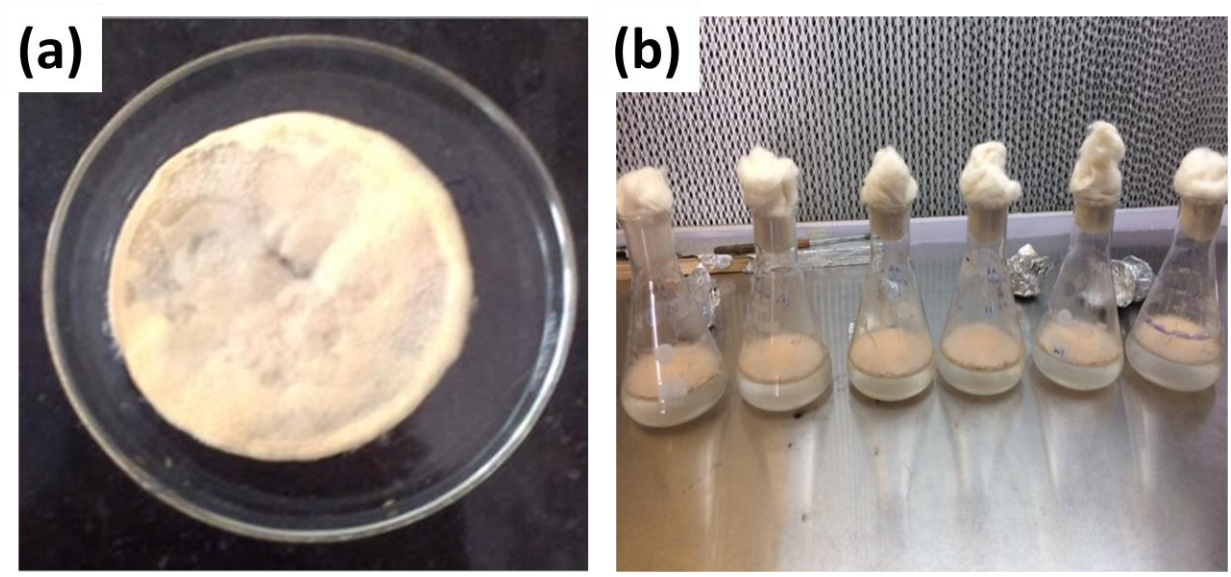

Figure 1 (a) Typical harvested biofilm (FBC) of diameter$\sim 8\ cm$, (b) Biofilms growing on the liquid interface.

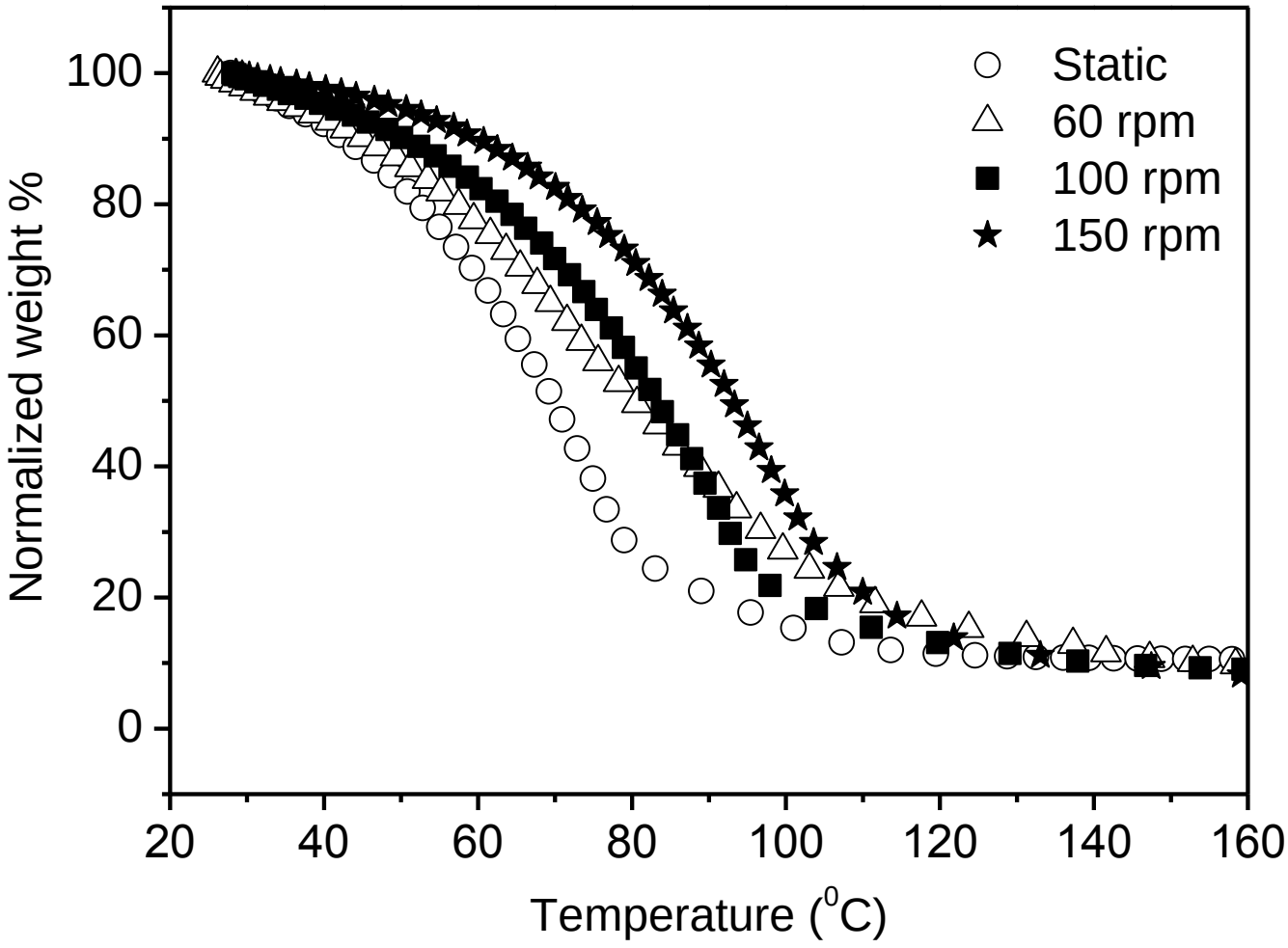

Figure 2 Plot from thermogravimetric analysis shows that all the FBCs lost more than 90% of their initial wet weight, in single step, before reaching 120^{0}C, indicating that they are mostly filled with water.

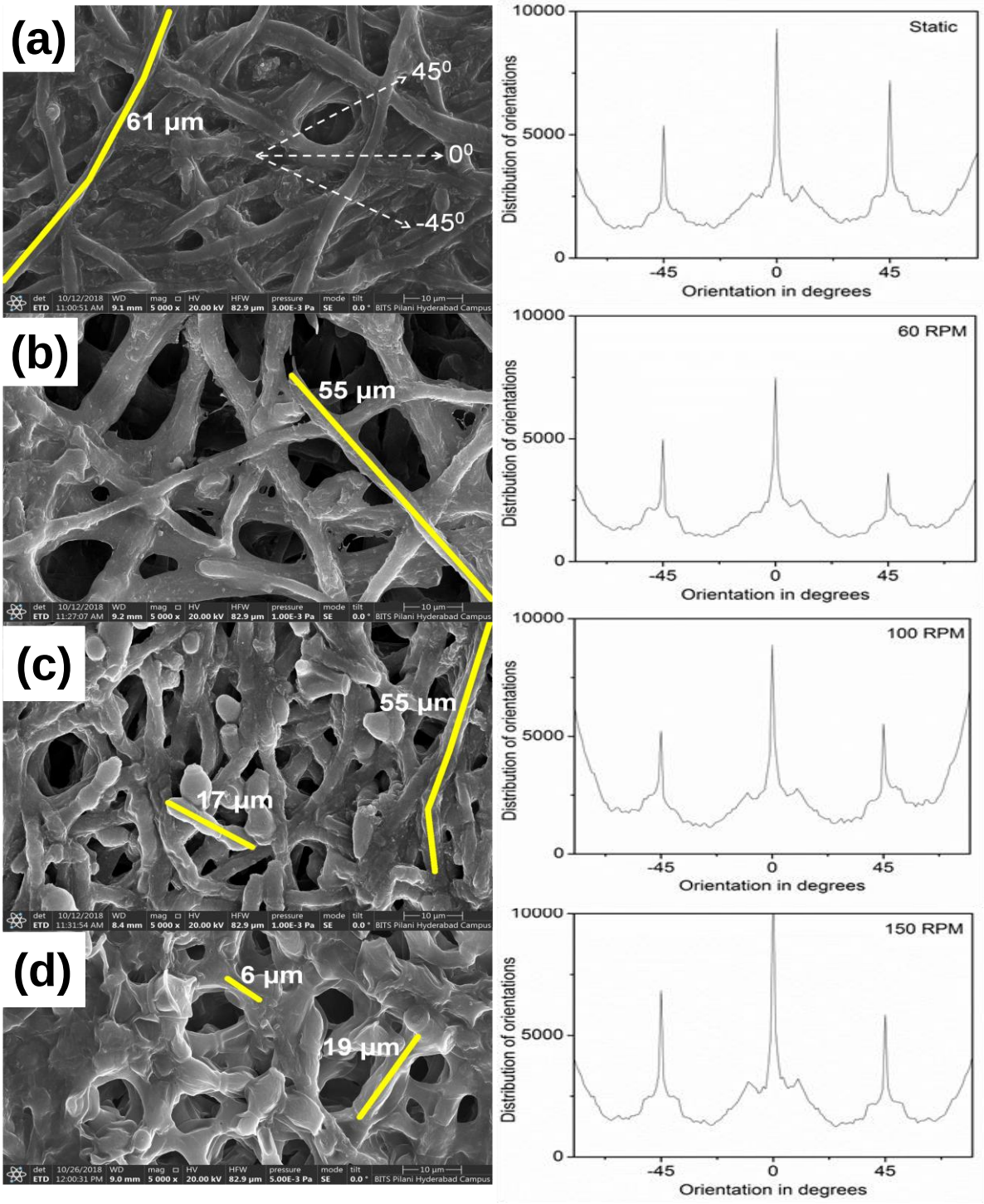

Figure 3 Representative FESEM images of the FBCs (*left*) and filament orientation distribution (*right*) for (a) static, (b) 60 RPM, (c) 100 RPM, (d) 150 RPM. In the FESEM images the dotted lines for the angles and the yellow colored curve on a few filaments are drawn for visually aid.

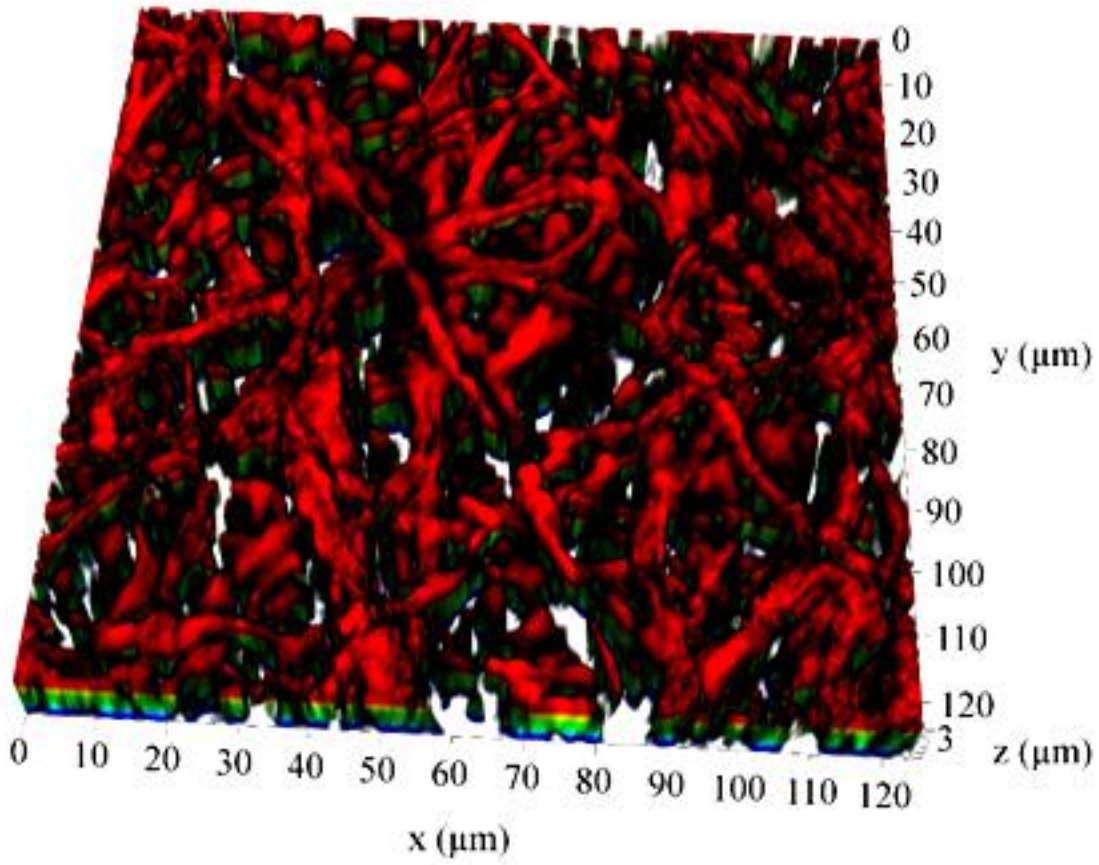

Figure 4 Three-dimensional reconstructed confocal image of a portion of a FBC shows filamentous biomass (cells and ECM) depicted by colored regions, and white spaces which are the micropores. In the z-direction color variation from blue to red represents an increase in height.

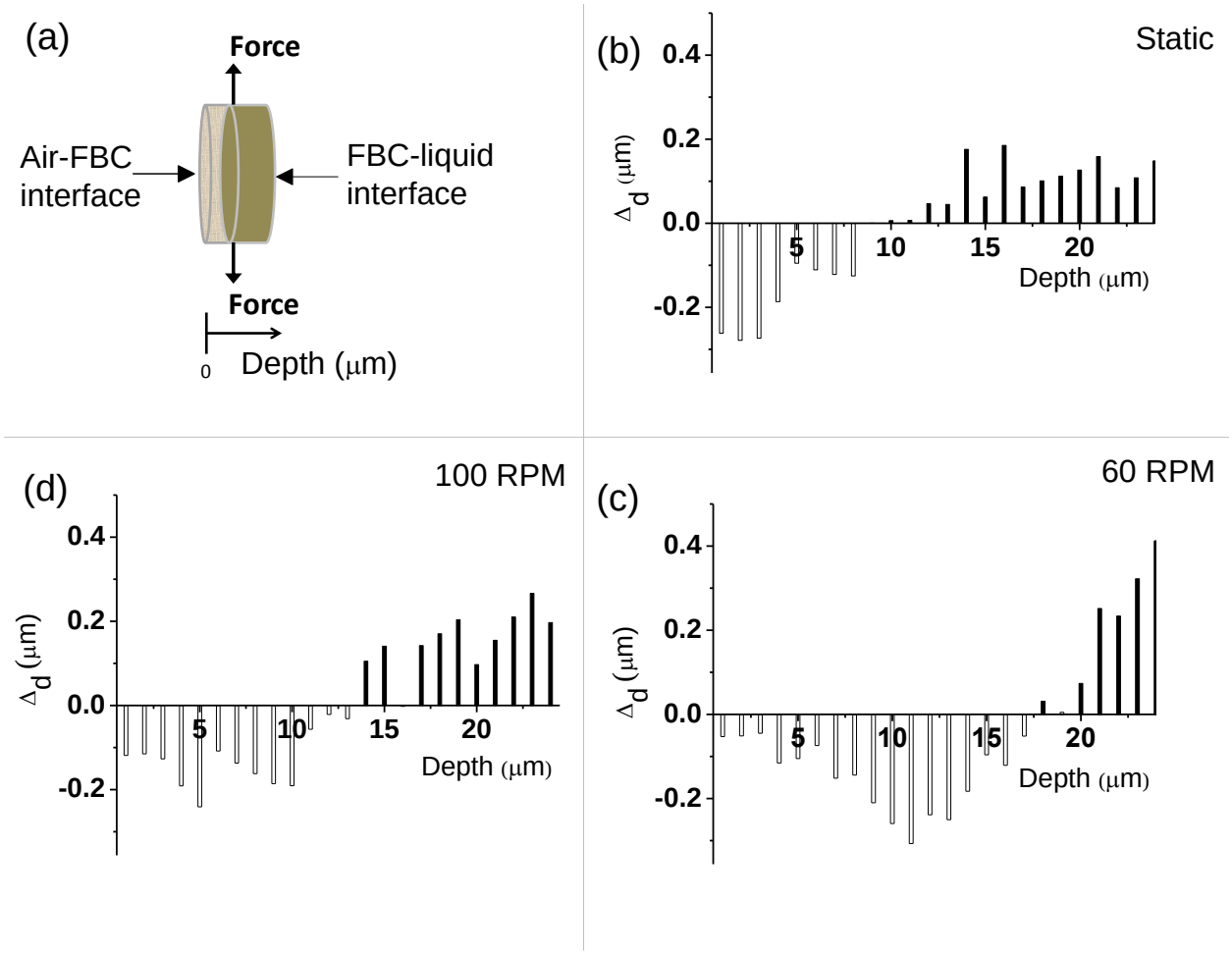

Figure 5 (a) Shows the orientation of the FBC while tensile loading, and (b)-(d) shows spatial heterogeneity - Δ_d, obtained by analysis of confocal images, for FBCs grown under static and agitated conditions. Unfilled bars representing $\Delta_d < 0$ pertain to ECM depleted region, and filled bars representing $\Delta_d > 0$ pertain to ECM-rich region. The spatial heterogeneities present in the sample converts the macroscopic tensile force into local shear forces.

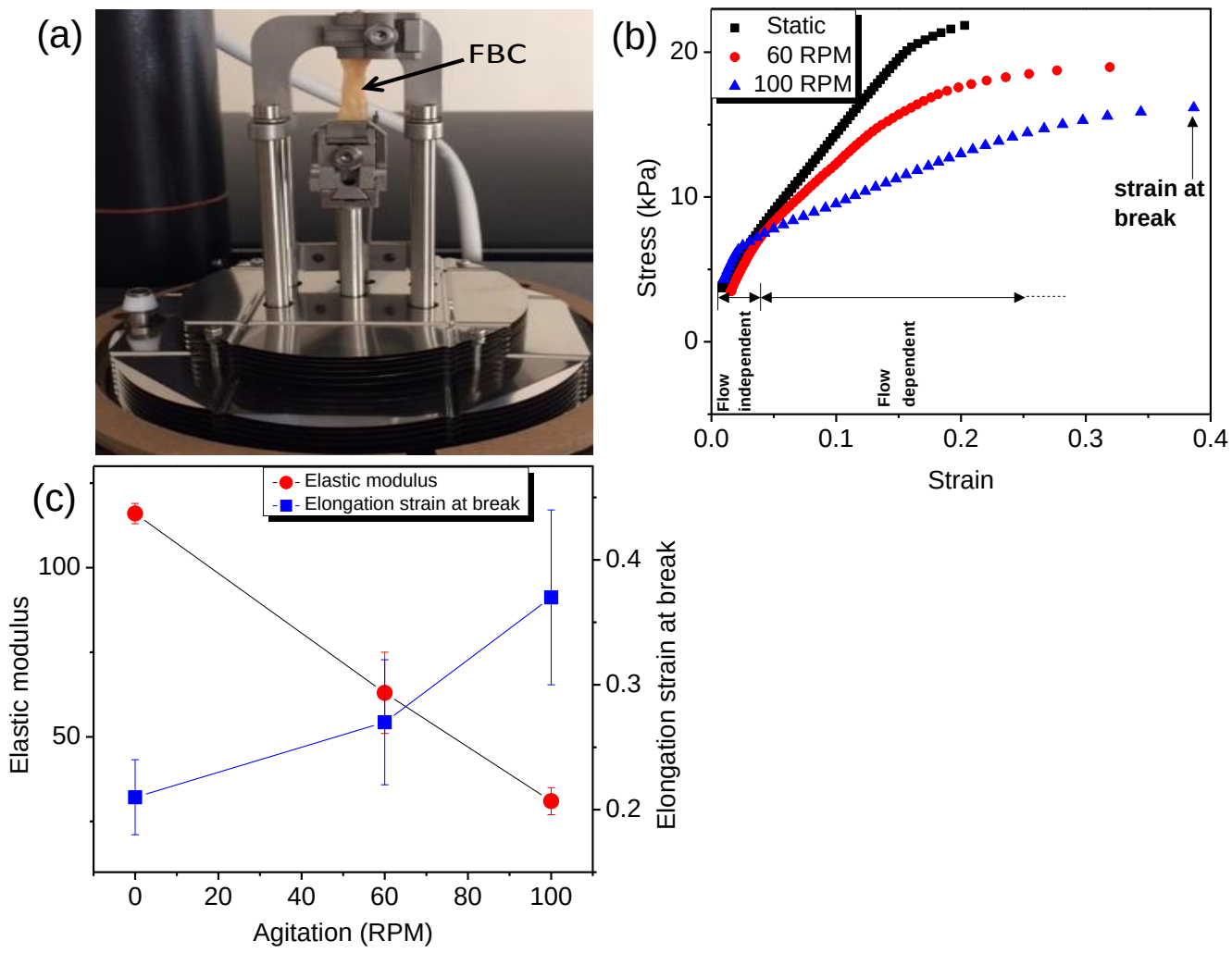

Figure 6 (a) A typical FBC loaded for mechanical testing, (b) Stress-strain curves for the FBCs grown under static and agitated conditions have a flow independent regime, and a flow dependent regime influenced by their water content, (c) dependence of elastic modulus and elongation strain at break on the agitated growth conditions of the FBCs.

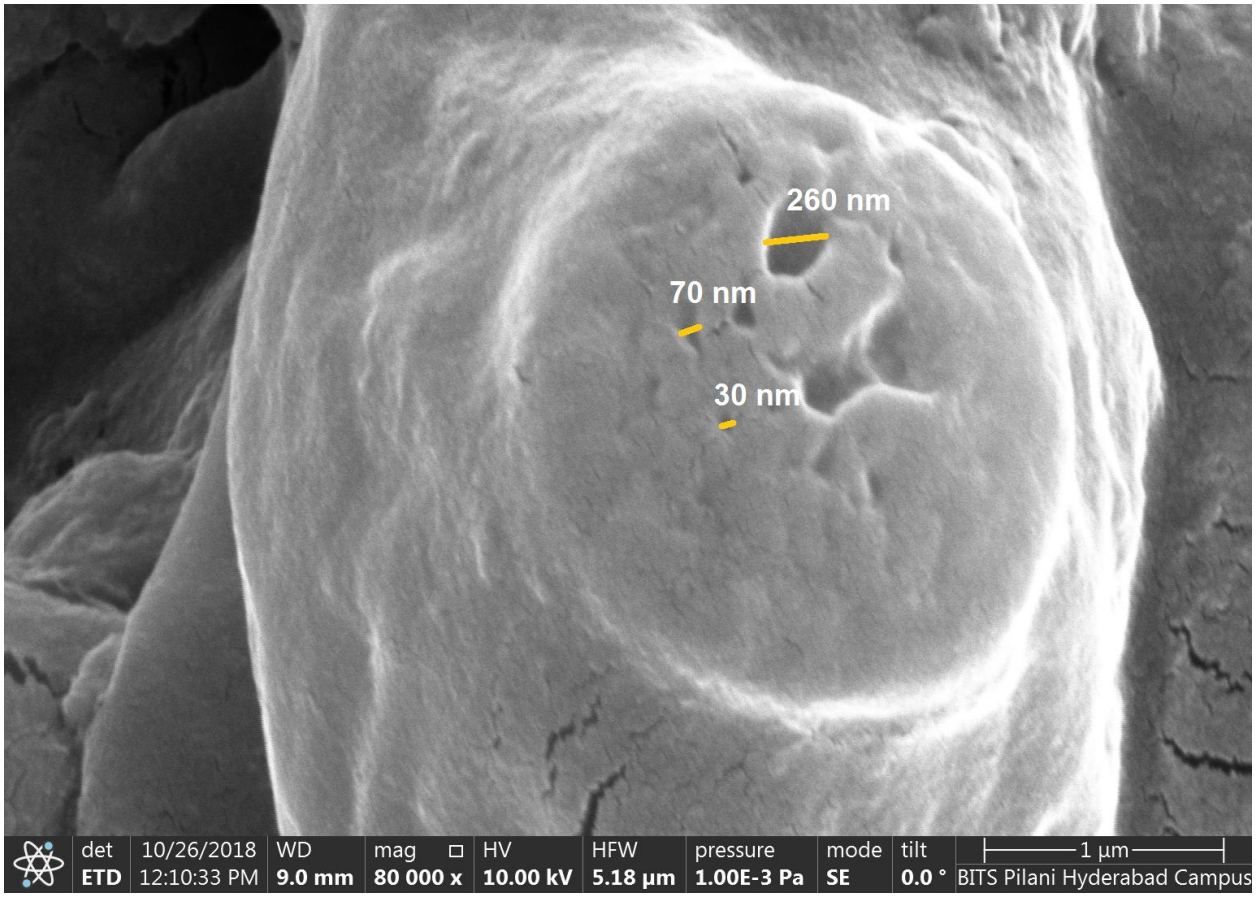

Figure 7 FESEM image showing nanopores in ECM as predicted by calculations assuming a pure entropic response of a cross-linked polymer.

Graphical abstract